Biogeosciences Discuss., https://doi.org/10.5194/bg-2017-448
Manuscript under review for journal Biogeosciences
Discussion started: 2 November 2017

Short-term fate of intertidal microphytobenthos carbon under enhanced nutrient availability: A ^{13}C pulse-chase experiment

Philip M. Riekenberg[1,a*], Joanne M. Oakes[1], Bradley D. Eyre[1]

[1]Centre for Coastal Biogeochemistry, Southern Cross University, PO Box 157, Lismore, NSW, 2480, Australia

[a]Present address: NIOZ Royal Netherlands Institute for Sea Research, Department of Marine Microbiology and Biogeochemistry, PO Box 59, 1790AB Den Burg

[*] Corresponding author: phrieken@gmail.com, (0031) 222 369 409

Keywords: benthic microalgae, bacteria, biomarker, nutrients

Running head: Intertidal carbon processing

Biogeosciences Discuss., https://doi.org/10.5194/bg-2017-448
Manuscript under review for journal Biogeosciences
Discussion started: 2 November 2017

ABSTRACT:

Shallow coastal waters in many regions are subject to nutrient over-enrichment. Microphytobenthos (MPB) can account for much of the carbon (C) fixation in these environments, depending on the depth of the water column, but the effect of enhanced nutrient availability on the processing and fate of MPB-derived C is relatively unknown. In this study, MPB were labeled (stable isotope enrichment) in situ using ^{13}C-sodium bicarbonate. The processing and fate of the newly-fixed MPB-C was then traced using ex situ incubations over 3.5 d under different concentrations of nutrients (NH_4^+ and PO_4^{3-}: ambient, 2× ambient, 5× ambient, and 10× ambient). After 3.5 d, sediments incubated with increased nutrient concentrations (amended treatments) had increased loss of ^{13}C from sediment organic matter as a portion of initial uptake (95% remaining in ambient vs 79-93% for amended treatments) and less ^{13}C in MPB (52% ambient, 26-49% amended), most likely reflecting increased turnover of MPB-derived C supporting increased production of extracellular enzymes and storage products. Loss of MPB-derived C to the water column via dissolved organic C was minimal regardless of treatment (0.4-0.6%). Loss due to respiration was more substantial, with effluxes of dissolved inorganic C increasing with additional nutrient availability (4% ambient, 6.6-19.8% amended). These shifts resulted in a decreased turnover time for algal C (419 d ambient, 134-199 d amended). This suggests that nutrient enrichment of estuaries may ultimately lead to decreased retention of carbon within MPB-dominated sediments.

Biogeosciences Discuss., https://doi.org/10.5194/bg-2017-448
Manuscript under review for journal Biogeosciences
Discussion started: 2 November 2017

1.0 Introduction

Intertidal sediments are important sites for the processing of carbon (C) within estuaries, producing, remineralizing, and transforming considerable amounts of organic material prior to its export to the coastal shelf (Bauer et al. 2013). Algal production is a key source of C within the coastal zone, and is primarily derived from microphytobenthos (MPB) in shallow photic sediments (Hardison et al. 2013; Middelburg et al. 2000). In addition to algal cells being a labile carbon source, MPB exude large amounts of carbohydrates as extracellular polymeric substances (EPS) (Goto et al. 1999) that allow for vertical migration and enhance sediment stability (Stal 2010). A better understanding of the carbon pathways utilized during processing of algal cells and exudates within sediments is important for determining the quality and quantity of carbon exported from estuarine waters to continental shelves.

Application of stable isotope tracers cause isotopic enrichments that usually serve to make negligible the variability associated with fractionation effects in natural abundance stable isotope techniques. As such, stable isotope tracers have been useful for elucidating pathways for the processing and loss of MPB-derived C within estuarine sediments. Loss pathways for MPB-derived C include resuspension (Oakes and Eyre 2014), fluxes of dissolved inorganic C (DIC) due to mineralization and respiration (Evrard et al. 2012; Oakes et al. 2012), fluxes of dissolved organic C (DOC) comprised of microbial exudates and products from cell lysis (Oakes et al. 2010a), and direct production of CO_2 (Oakes and Eyre 2014). Stable isotope tracer studies have also enabled quantification of the trophic transfer (Middelburg et al. 2000; Miyatake et al. 2014; Nordström et al. 2014; Oakes et al. 2010a) and

flux of newly produced C from sediments (Andersson et al. 2008; Oakes et al. 2012; Van Nugteren et al. 2009).

When ^{13}C is combined with analysis of phospholipid-linked fatty acids (PLFAs), it becomes possible to trace C transfer into individual microbial groups that account for the living biomass within sediment organic C (OC) (Drenovsky et al. 2004; Hardison et al. 2011; Oakes et al. 2012; Oakes and Eyre 2014; Spivak 2015). This allows for the quantification of microbial transfers of newly produced algal C between MPB and bacteria and the relative contributions of MPB and bacteria to microbial biomass in sediment OC. This technique has shown that EPS produced by MPB is readily utilized as a C source for heterotrophic bacteria (Oakes et al. 2010; van Oevelen et al. 2006). Pathways for processing of MPB-derived C have been reasonably well described, but the response of these pathways to local environmental changes remains a significant knowledge gap.

A major source of environmental change in coastal systems is nutrient over-enrichment (Cloern et al. 2001), which may affect the assimilation and flux pathways of MPB-derived carbon through 1) increased microbial biomass resulting from relaxation of nutrient limitation, 2) increased algal production that drives elevated heterotrophic processes as bacteria utilize newly produced C, and 3) increased loss of C as DIC via respiratory pathways as heterotrophic processes dominate. MPB are able to use both porewater and water column nutrients, and although MPB biomass can increase with elevated nutrient availability (Armitage and Fong 2004; Cook et al. 2007), this is not always the case, with multiple studies finding no corresponding increase in MPB biomass (Alsterberg et al. 2012; Piehler et al. 2010; Spivak and Ossolinski 2016). Processing and mineralization of C are significantly affected by changes in the relationship between MPB and bacteria (Evrard et al. 2012). Both EPS

79 production and bacterial utilization of newly produced EPS may decrease with increasing
80 nutrient availability (Cook et al. 2007). Increased autochthonous production driven by nutrient
81 enrichment can lead to increased heterotrophy, as newly produced organic matter is
82 mineralized (Fry et al. 2015), resulting in increased DIC production. Increased
83 remineralization of newly produced MPB-C will result in greater loss of DIC from intertidal
84 sediment via bacterial respiration (Hardison et al. 2011).

85 In this ^{13}C pulse-chase study we aimed to quantify the processing pathways of MPB-
86 derived C within subtropical intertidal sediments and to determine how this is affected by
87 increased nutrient loading. The in situ MPB community was used to provide a pulse of labeled
88 MPB-C of similar quantity and quality to normal production. Even application of separate
89 label applications for each plot prior to incubation served to isolate the subsequent effect of
90 increased nutrient availability on the processing of MPB-derived C. Pathways considered
91 included transfer through sediment compartments (MPB, bacteria, uncharacterized and
92 sediment OC), and loss via fluxes of DOC and DIC. We expected increased nutrient
93 availability to stimulate MPB production of EPS after initial labeling, resulting in decreased
94 turnover times for MPB-C as well as a shift towards dominance of heterotrophic processes as
95 bacteria utilize this additional labile C. We further hypothesized that enhanced heterotrophy
96 would increase loss of newly fixed algal-derived C via respiration as $DI^{13}C$. Incorporation of
97 ^{13}C into biomarkers should reflect the shift towards heterotrophy, with quicker shifts towards
98 increased bacterial utilization of newly produced algal C corresponding with increased
99 nutrient load. Both DIC and DOC should be significant loss pathways for newly produced
100 algal C as labile OM is readily processed by heterotrophs.

101 **2.0 Methods**

Biogeosciences Discuss., https://doi.org/10.5194/bg-2017-448
Manuscript under review for journal Biogeosciences
Discussion started: 2 November 2017

2.1 Study site

The study site was a subtropical intertidal shoal ~ 2 km upstream of the mouth of the Richmond River estuary in New South Wales, Australia (28˚52'30"S, 153˚33'26"E). The 6900 km^2 catchment has an annual rainfall of 1300 mm (McKee et al. 2000) and an average flow rate of 2200 ML d^{-1} (daily gauged flow adjusted for catchment area, averaged over years for which data was available; 1970–2013). Although the Richmond River Estuary has highly variable flushing, salinity, and nutrient concentrations associated with frequent episodic rainfall events and flooding (Eyre 1997; Mckee et al. 2000), this study was undertaken during a dry period. The site experiences semidiurnal tides with a range of ~2 m. Samples were collected in summer January 2015 with average site water temperature of 25.6 ± 2.3°C. Sediment at depths of 0-2 cm, 2-5 cm and 5-10 cm was dominated by fine sand (66%-73%), and sediment across 0-10 cm had an organic C content of 17.5 ± 0.02 mol C m^{-2}. Sediment molar C:N was lowest at 2-5 cm, but comparable across all other depths (top scrape (TS) 14.4 ± 1.6, 0-2 cm 17.2 ± 1.7, 2-5 cm 10.9 ± 0.5, 5-10 cm 16.2 ± 2.2).

2.2 Overview

We labeled MPB with ^{13}C via in situ application of ^{13}C-labeled sodium bicarbonate to exposed intertidal sediments. Unincorporated ^{13}C was flushed from the sediment during the next tidal inundation of the site. Sediment cores were collected and incubated in the laboratory over 3.5 d under four nutrient enrichment scenarios (ambient, minimal, moderate, and elevated) using pulsed nutrient additions. Incubation of cores ex situ allowed for explicit control of nutrient additions and examination of the short-term processing and fate (loss to overlying water) of MPB carbon. Sediments remained inundated during incubations with minimal water exchange, as might be expected during neap tide at this site. Inundation also

Biogeosciences Discuss., https://doi.org/10.5194/bg-2017-448
Manuscript under review for journal Biogeosciences
Discussion started: 2 November 2017

served to minimize C loss via physical resuspension and export while we were examining sediment processing.

2.3 ^{13}C-labeling

Bare sediment within a 2 m^2 experimental plot was ^{13}C-labeled when sediments were first exposed during the ebbing tide in the middle of the day by using motorized sprayers to evenly apply 99% $NaH^{13}CO_3$ onto individual 400 cm^2 subplots, closely following the method outlined in Oakes and Eyre (2014). Label applications were prepared using NaCl-amended Milli-Q matching site salinity (34.6), and 20 ml aliquots (1.7 mmol ^{13}C) were applied to each individual subplot, resulting in application of 42.5 mmol ^{13}C m^{-2}. The use of individual aliquots of label ensured even ^{13}C application across the sediment surface. Assimilation of label by the sediment community occurred over ~4 hours with average light exposure of 1376 µE m^{-2} s^{-1}, before tidal inundation removed the majority of unincorporated ^{13}C. Removal was confirmed by loss of 99.0% of the applied ^{13}C from treatment applications within initial cores sampled in the field.

2.4 Collection of sediment cores

Prior to label application, 3 cores (9 cm diameter, 20 cm depth) were collected from unlabeled sediment surrounding the treatment plots and immediately extruded and sectioned (0-0.2 cm (top scrape, TS), 0.2-2 cm, 2-5 cm, and 5-10 cm) to provide control natural abundance sediment OC δ^{13}C values for sediment depths within the study site. Eleven hours after label application, at low tide, 35 sediment cores were similarly collected from the labeled plot using Plexiglas core liners. Immediately, three cores were extruded and sectioned as above to determine initial ^{13}C uptake and grain size distribution for all sediment depths, and chlorophyll-α (Chl-α) concentrations in 0-1 cm sediments. All samples were placed within

Biogeosciences Discuss., https://doi.org/10.5194/bg-2017-448
Manuscript under review for journal Biogeosciences
Discussion started: 2 November 2017

plastic zip-lock bags, transported to the laboratory on ice, and stored frozen in the dark (-20 ° C). Plexiglas plates were used to seal the bottom of the core liners, and cores for incubation were then transported to the laboratory within 2 hours of sampling. Site water (400 L) was collected and transported to the laboratory for use in incubations.

2.5 Nutrient amendment

Pulsed applications of nutrients for each treatment amendment were used to mimic a range of nutrient concentrations without exceeding sediment capacity for uptake. The treatment tanks were set up at ambient concentration (site water, DIN of 2.5 ± 0.04 µmol N L^{-1}, measured on incoming tide), and with N (NH_4^+) and P (H_3PO_4) amendment to site water at 2× (minimal treatment), 5× (moderate treatment) and 10× (elevated treatment) average water column concentrations near the study site (4 µmol L^{-1} NH_4^+ and 5 µmol L^{-1} PO_4^{3-}; Eyre (1997; 2000). To allow thorough mixing, the initial pulse of nutrients was added to both incubation tanks and bags holding replacement water for sampling, one hour prior to cores being transferred into the incubation tanks. An additional pulse of NH_4^+ was applied to incubation tanks at 1.5 d (after sample collection) to mimic the nutrient availability that occurs with regular inundation of tidal sediments. Silica (Si) was also added to all incubation tanks at 2.5 d (after sample collection) to ensure that isolation of the benthic diatom-dominated sediment from regular water turnover did not result in secondary limitation of Si. There was no significant accumulation of NH_4^+ within treatment tank water, as nutrients were readily processed (Supplemental Fig. 1).

2.6 Benthic flux incubations

In the laboratory, cores were fitted with magnetic stir bars positioned 10 cm above the sediment surface, filled with ~2 L of site water, and randomly allocated to one of the four 85

L treatment tanks (Ambient, Minimal, Moderate, Elevated; eight cores per treatment). Water in the treatment tanks and cores was continuously recirculated, held at in situ temperature (25 ± 1°C) by a chiller on each tank, and aerated. Cores were stirred via a rotating magnet at the center of each treatment tank, which interacted with the magnetic stir bars. Stirring occurred at a rate below the threshold for sediment resuspension (Ferguson et al. 2003). Three sodium halide lamps suspended above the treatment tanks provided 824 ± 40 µE m^{-2} s^{-1} to the sediment/water interface within the cores on a 12 h light/12 h dark cycle which approximated the average light level measured at the sediment surface during inundation (941.4 ± 139 µE m^{-2} s^{-1}). Cores were allowed to acclimate in tanks for 6 h prior to the start of incubation. Cores remained open to the tank water until 30 min before sampling, when clear Plexiglas lids were fitted to each core liner to seal in overlying water within the core for the duration of the incubation (~16 h). Dissolved oxygen (± 0.01 mg L^{-1}) and pH (± 0.002 pH) were measured optically and electrically (Hach HQ40d multi-parameter meter) via a sampling port in the lid. Initial samples were taken 30 min after closure of the lids, dark samples were taken after ~12 hours incubation with no light, and light samples were taken after 3 hours of illumination following the end of the dark period. During sampling, 50 ml of water was syringe-filtered (precombusted GF/F) into precombusted 40 ml glass vials with Teflon coated septa, killed with $HgCl_2$ (20 µL saturated solution), and refrigerated prior to analysis for concentration and $\delta^{13}C$ of DIC and DOC. Sample water was simultaneously replaced by water held in replacement bags as sampling occurred at each time point. No samples were collected for analysis of gaseous CO_2 fluxes from exposed sediments, as this was previously determined to be a negligible pathway for loss of MPB-C at this site (Oakes and Eyre 2014). At the end of sampling for the light period, cores were extruded, sectioned and sampled for Chl-α in the

Biogeosciences Discuss., https://doi.org/10.5194/bg-2017-448
Manuscript under review for journal Biogeosciences
Discussion started: 2 November 2017

same manner as control cores and stored frozen (-20°C). Eight cores (two cores per treatment) were sampled in this manner for water column fluxes, PLFAs, and sediment OC after 1.5 d, 2.5 d and 3.5 d of incubation. Additionally, 8 cores (two cores per treatment) were sampled for only PLFAs and sediment OC at 0.5 d of incubation.

2.7 Sample analysis

Chl-*α* was measured by colorimetry (Lorenzen 1967) for each core (0-1 cm depth). MPB-C biomass was calculated assuming a C:Chl-*α* ratio of 40, within the range reported for algae in Australian subtropical estuaries (30-60 Ferguson et al. 2004; Oakes et al. 2012). Biomass measurements utilizing Chl-α were used to compare biomass across controls and treatments and were not utilized in calculations for uptake of ^{13}C into MPB or bacteria using PLFAs. Bacterial C biomass for controls was estimated based on MPB-C biomass derived from Chl-α and the ratio of MPB to bacterial biomass obtained from PLFA analysis of the control cores (n=3).

Sediment samples were lyophilized, loaded into silver capsules, acidified (10% HCl), dried (60°C to constant weight), and analyzed for %C and $\delta^{13}C$ using a Thermo Flash Elemental Analyzer coupled to a Delta V IRMS via a Thermo ConFlo IV. Samples were run alongside glucose standards that are calibrated against international standards (NBS 19 and IAEA ch6). Precision for $\delta^{13}C$ was 0.1‰ with decreasing precision for enrichments above 100‰.

PLFAs specific to bacteria (i + a 15:0) were used as biomarkers for this group. However, although visual analysis confirmed the presence of a large number of pennate diatoms at the study site and diatom-specific PLFAs (e.g. 20:5(n-3)) were detected,

chromatographic peaks for these PLFAs were sometimes indistinct. The 16:1(n-7) PLFA, which represents 27.4% of total diatom PLFAs (Volkman et al. 1989), was therefore used as a biomarker for diatoms, following correction for contributions from gram-negative bacteria and cyanobacteria as described below and in Oakes et al. (2016), as it was consistently present across all samples. Extraction of PLFAs used 40 g of freeze-dried sediment and a modified Bligh and Dyer technique. Sediment was spiked with an internal standard (500 µL of 1 mg ml^{-1} tridecanoic acid, C_{13}), immersed in 30-40 ml of a 3:6:1 mixture of dichloromethane (DCM), methanol, and Milli-Q water, sonicated (15 min), and centrifuged (15 min, 9 *g*). The supernatant was removed into a separating funnel and the pellet was re-suspended in 30-40 ml of the DCM:MeOH:Milli-Q mixture, sonicated, and centrifuged twice more to ensure complete removal of biomarkers. DCM (30 ml) and water (30 ml) were added to the supernatant, gently mixed, and phases were allowed to separate prior to removal of the bottom layer into a round bottom flask. The top layer was then rinsed with 15 ml of DCM, gently shaken, and phases allowed to separate prior to addition to the round bottom flask. This extract was then concentrated under vacuum and separated using silica solid phase extraction columns (Grace; 500 mg, 6.0 ml) by elution with 5 ml each of chloroform, acetone, and methanol. The fraction containing methanol was retained, reduced to dryness under N_2, methylated (3 ml 10:1:1 MeOH:HCl:$CHCl_3$, 80 °C, 2 h), quenched using first 3 ml and then 2 ml of 4:1 hexane:DCM, evaporated to ~ 200 µl under N_2, transferred to a GC vial for analysis, and stored frozen (-20 °C). PLFA concentrations and $\delta^{13}C$ values were measured using a non-polar 60 m HP5-MS column in a Trace GC coupled to a Delta V IRMS with a Thermo Conflo III interface following the protocol outlined in Oakes et al. (2010a).

Biogeosciences Discuss., https://doi.org/10.5194/bg-2017-448
Manuscript under review for journal Biogeosciences
Discussion started: 2 November 2017

DIC and DOC concentrations and $\delta^{13}C$ values were measured via continuous-flow wet oxidation isotope-ratio mass spectrometry using an Aurora 1030W total organic C analyzer coupled to a Thermo Delta V isotope ratio mass spectrometer (IRMS) (Oakes et al. 2010b). Sodium bicarbonate (DIC) and glucose (DOC) of known isotopic composition dissolved in He-purged Milli-Q were used to correct for drift and verify both concentration and $\delta^{13}C$ of samples. Reproducibility was ± 0.2 mg L^{-1} and ± 0.1 ‰ for DIC and ± 0.2 mg L^{-1} and ± 0.4 ‰ for DOC.

2.8 Calculations

Incorporation of ^{13}C into sediment OC, bacteria, and MPB (mmol ^{13}C m^{-2}) was calculated as the product of excess ^{13}C (fraction ^{13}C in sample – fraction ^{13}C in control) and the mass of OC within each pool. For sediment, OC was the product of %C and dry mass per unit area.

Excess ^{13}C for PLFAs was determined only for 0-2 cm, 2-5 cm, and 5-10 cm depths, as there was inadequate sample mass for the 0-0.2 cm top scrape. Due to limitations of time and cost, PLFA samples were taken from only one of the two cores incubated for each treatment at each sampling period. PLFA excess ^{13}C for both bacteria and diatoms was the product of excess ^{13}C contained in the PLFA (fraction ^{13}C in PLFA in sample – fraction ^{13}C in PLFA in control) and the concentrations of C within respective biomarkers. Concentrations of PLFA C were calculated from their peak areas relative to the internal C_{13} standard spike. Biomass of diatoms and bacteria were calculated using the method described by Oakes et al. (2016). Briefly, bacterial biomass was calculated as:

1. $Biomass_{bacteria} = Biomass_{i+a15:0} / (a \times b)$

Biogeosciences Discuss., https://doi.org/10.5194/bg-2017-448
Manuscript under review for journal Biogeosciences
Discussion started: 2 November 2017

where *a* represents the average concentration of PLFA (0.056 g C PLFA per g C biomass; Brinch-Iversen and King 1990) in bacteria and *b* represents the average fraction of PLFA accounted for by i+a15:0 within bacteria-dominated marine sediments (0.16, Osaka Bay, Japan; Rajendran et al. 1994; Rajendran et al. 1993). Biomass estimates for bacteria calculated using the minimum and maximum fraction values (16-19% for i+a15:0; Rajendron et al. 1993) resulted in a 16% difference.

For diatoms, a mixing model was used to correct the concentration and $\delta^{13}C$ value of 16:1(n-7) for the any contribution from non-diatom sources. Due to the scarcity of cyanobacteria observed using light microscopy (1000×), low sediment D-/L- alanine ratios measured previously at this site (as low as 0.0062, Riekenberg et al. 2017), and lack of the characteristic 18:2(n-6) peak (Bellinger et al. 2009) cyanobacteria were assumed to make a negligible contribution to the 16:1(n-7) peak. A two-source mixing model was applied to correct the concentration and $\delta^{13}C$ value of the 16:1(n-7) peak for the contribution of gram-negative bacteria, based on a typical ratio of 18:1(n-7) to 16:1(n-7) for gram-negative bacteria of 0.7 (Edlund et al. 1985) as previously applied in Oakes et al. (2016). Biomass for diatoms was calculated using the formula:

2. $\text{Biomass}_{\text{Diatom}} = \text{Biomass}_{\text{corrected16:1(n-7)}} / (c \times d)$

where *c* is the average fraction of diatom PLFAs accounted for by corrected 16:1(n-7) (0.67; Volkman et al. 1989) and *d* is the average PLFA concentration in diatoms (0.035 g PLFA C per g of C biomass; Middelburg et al. 2000). Biomass estimates for diatoms calculated using maximum and minimum fraction values for 16:1(n-7) (18-33%; Volkman et al. 1989) were within 50% of estimates based on the average value.

Fluxes across the sediment-water interface were calculated as a function of incubation time, core water volume and sediment surface area. Dark flux rates were calculated using concentration data from the dark incubation period and light flux rates from the light incubation period. The following parameters were calculated from dark and light rates:

3. Respiration (R) = Dark DO flux h^{-1}
4. Net primary production (NPP) = Light DO flux h^{-1}
5. Gross primary production (GPP) = NPP + R
6. Production/respiration (P/R) = GPP x daylight hours (12 h) / R x 24 h (Eyre et al. 2011)

Total ^{13}C in DIC and DOC (µmol ^{13}C) in the overlying water in the sediment core was calculated for initial, the end of the dark period, and the end of the light period as the product of excess ^{13}C (excess ^{13}C in labeled sample versus relevant natural abundance control), core volume, and concentration. Total excess flux of ^{13}C as DIC or DOC (µmol ^{13}C m^{-2} h^{-1}) was then calculated as:

7. Excess ^{13}C flux = (Excess $^{13}C_{start}$ – Excess $^{13}C_{end}$) / SA / *t*

where excess $^{13}C_{start}$ and excess $^{13}C_{end}$ represent excess ^{13}C of DIC or DOC at the start and end of dark and light incubation periods, SA is sediment surface area, and *t* is incubation period length (h). Net fluxes of excess ^{13}C (excess ^{13}C m^{-2} h^{-1}) for DIC and DOC were calculated as:

8. Net flux = ((dark flux * dark hours) + (light flux * light hours))/ 24 hours

Total ^{13}C lost via flux to the water column from initial labeling to each sampling period was interpolated from measured net flux values by calculating the area underneath the curve for

each treatment. To prevent the potential development of limitations during incubations, O_2 concentrations were not allowed to drop below 60% saturation in the dark and light incubations were shortened (~3 h) to ensure that production was not limited due to available resources within limited core volume.

2.9 Data Analysis

MPB-C biomass was determined using chl-a data for cores within all treatments for 0.5 d, 1.5 d, 2.5 d and 3.5 d. We therefore used a two-way analysis of variance (ANOVA) to determine whether MPB-C biomass was affected by treatment and/or time. P/R ratios were determined for 1.5 d, 2.5 d and 3.5 d to determine whether significant differences occurred between treatments within each time period ($\alpha = 0.05$). Levene's tests indicated that variances were homogeneous in all cases and there were no significant interactions between variables in either analysis. For significant effects of treatment or time, post hoc Tukey tests were used to identify significant differences between groups.

Total uptake for ^{13}C into both MPB and bacteria, and relative ^{13}C uptake into MPB were determined for only a single core across all treatments from 0.5 d, 1.5 d, 2.5 d and 3.5 d. To increase replication for statistical analysis, and therefore increase the power to detect a significant difference, we therefore grouped data across times into two levels: before 1.5 d (including 0.5 d and 1.5 d) and after 1.5 d (including 2.5 d and 3.5 d). There was no pooling of data across treatments. A two-way ANOVA was then used to determine whether significant differences occurred among treatments within each pooled time period ($\alpha = 0.05$). No significant interactions were observed for total uptake into MPB or bacteria, but there was a significant interaction observed for relative ^{13}C uptake into MPB. For significant effects of

interaction, treatment, time, post hoc Tukey tests were used to identify significant differences between groups.

The ^{13}C remaining in microbial biomass and sediment OC were fitted with an exponential decay function for each treatment across 3.5 d. Loss rate constants for these exponential relationships were compared across treatments and are reported as positive numbers following mathematical conventions associated with loss rates.

3.0 Results

3.1 Uptake of nutrient additions

Uptake of the added nutrients into the sediment was rapid and substantial, as indicated by decreases in dissolved inorganic nitrogen ($NH_4^+ + NO_x$) concentrations in the overlying core water to $<1.2 \pm 0.1$ µM L^{-1} by 0.5 d. Across the incubation periods, elevated DIN concentrations in overlying water were occasionally observed (Supplemental Fig. 1), but corresponded with times when the cores were sealed for light and dark incubations, indicating that DIN production was a result of in-core processing rather than nutrient amendments.

3.2 Sediment characteristics

Control sediment OC content was greater in the 2-5 cm depth (187.5 ± 27.7 µmol C g^{-1}) than at all other sediment depths (112.3 ± 11.4 µmol C g^{-1} in the TS, 149.8 ± 31.6 µmol C g^{-1} at 0-2 cm, and 120.1 ± 16.5 µmol C g^{-1} at 5-10 cm). Natural abundance $\delta^{13}C$ values were most enriched in surface sediments (-18.7‰ in TS) and became progressively depleted within deeper sediments to -22.1‰ at 5-10 cm (Table 1). In the 0-2 cm depth of the control sediment,

Biogeosciences Discuss., https://doi.org/10.5194/bg-2017-448
Manuscript under review for journal Biogeosciences
Discussion started: 2 November 2017

345 MPB-C biomass was 321.9 ± 42.0 mmol C m^{-2} and bacterial biomass was 500.4 ± 65.3 mmol
346 C m^{-2} (Table 1).

347 **3.3 Initial ^{13}C uptake**

348 Uptake of ^{13}C into sediment OC occurred rapidly and was observed in the first
349 cores collected (11 h after labeling, after tidal flushing, and with cores sectioned in the field).
350 At this time, prior to laboratory incubation and nutrient amendment, 1549 ± 140 µmol ^{13}C m^{-2}
351 had been incorporated into sediment OC. Sediment OC was ^{13}C-enriched across all sediment
352 depths at this time (Table 1), but 78% of the initially incorporated ^{13}C was in the uppermost 2
353 cm of sediment (compared to 12.8% 2-5 cm, 9.4% 5-10 cm). Prior to incubation, ^{13}C uptake
354 into microbial biomass at 0-2 cm was dominated by MPB (92.7 ± 1.6%), despite their lower biomass
355 (200.2 ± 26.5 mmol C m^{-2}) compared to bacteria (311.3 ± 56.4 mmol C m^{-2}) within the labeled cores.
356 Conversely, bacteria dominated ^{13}C uptake in 2-5 cm sediment (66.8 ± 17.2% of the ^{13}C
357 within microbial biomass). Although sediment OC at 5-10 cm was ^{13}C-enriched, minimal
358 uptake was detected in microbial biomarkers.
359
360 **3.4 Effect of nutrient additions on P/R**

361 Average MPB biomass remained similar across treatments over the 3.5 d incubation
362 (two-way ANOVA: treatment $F_{3,31}$= 0.04, p=0.99; time $F_{3,31}$= 0.1, p=0.94, Supplemental
363 Figure 2). However, there were changes in P/R ratio that varied among treatments.
364 Examination of the effects of treatment and time on P/R showed no significant differences
365 (two-way ANOVA: treatment $F_{3,23}$=3.0, p=0.08; time $F_{2,23}$=2.7, p=0.11), although the post
366 hoc Tukey comparison between ambient and elevated treatments was nearly significant

(p=0.0506). For the ambient, minimal and moderate treatments, P/R ratios were dominated by autotrophy and changed little over the first 2.5 d (1.5 ± 0.8, 1.2 ± 0.4, and 1.3 ± 0.1, respectively, Fig. 1b) as any increases in production were offset by increased respiration (Fig. 1a). By 3.5 d the minimal treatment had shifted into heterotrophy (0.6 ± 0.1) as a result of increased respiration and decreased production., whereas P/R ratios for the ambient and moderate treatments remained essentially unchanged (1.3 ± 0.2, 1.3 ± 0.4). P/R in the elevated treatment was initially high compared to all other treatments (2.2 ± 0.2 at 0.5 d) indicating strong dominance of autotrophic production (Fig. 1a & B). However, P/R in the elevated treatment generally decreased to 1.1 ± 0.4 after 3.5 d (Fig. 1), indicating a strong shift away from autotrophy and towards dominance of heterotrophic processes as respiration increased and production decreased (Fig. 1a).

3.5 Incorporation of ^{13}C into sediment organic carbon

3.5.1 Uptake of ^{13}C into 0-2 cm sediment

At 0.5 d, the ^{13}C incorporated into sediment OC was predominantly contained in the 0-2 cm depth across all treatments (~65%-90%, Fig. 2) and was statistically similar across treatments (one-way ANOVA: $F_{3,7}$= 4.2, p=0.1). By 3.5 d, ^{13}C retention was lower within sediment from nutrient amended treatments compared to the ambient treatment. Whereas the ^{13}C contained in the 0-2 cm depth in the ambient treatment was similar across 3.5 d (78.9 ± 8.8% 1.5 d, 77.0 ± 16.4% 2.5 d, 81.6 ± 4.4% 3.5 d), the ^{13}C content decreased in the minimal, moderate and elevated treatments to 70.3 ± 8.3%, 73.6 ± 16.4%, and 68.8 ± 7.6%, respectively (Fig. 2).

Biogeosciences Discuss., https://doi.org/10.5194/bg-2017-448
Manuscript under review for journal Biogeosciences
Discussion started: 2 November 2017

3.5.2 Downward transport below 2 cm

Downward transport of newly labeled material to 2-5 cm depth was low across all treatments, but was higher for the elevated treatment at both 0.5 and 2.5 d. At 0.5 d there was less downward transport in minimal and moderate treatments compared to the ambient and elevated treatments. By 2.5 d downward transport was similar for ambient, minimal and moderate treatments (10%, 9%, 10%, respectively; Fig. 2), but was considerably higher in the elevated treatment (28.4%). By 3.5 d, ^{13}C incorporation into 2-5 cm sediment OC was similarly low for ambient, minimal and moderate treatments (8.0 ± 2.1%, 11.1 ± 0.1%, and 8.7 ± 2.1%, respectively), but lower in the elevated treatment (4.8 ± 2.1%). At 0.5 d, downward transport into the 5-10 cm layer was a relatively small portion of initial ^{13}C, but was higher in ambient and minimal treatments (8.7 ± 2.4% and 11.6 ± 1.5%) when compared to moderate and elevated treatments (2.3 ± 1.9% and 6.8 ± 0.1%, Fig. 2). Downward transport below 5 cm was similar (5-11%) for all treatments at 2.5 d and 3.5 d.

3.6 ^{13}C distribution amongst sediment compartments

3.6.1 Microbial biomass

The total ^{13}C content of MPB (mmol ^{13}C m^{-2}; Fig. 4a) decreased significantly from before 1.5 d to after 1.5 d for all treatments (two-way ANOVA: $F_{1,8}$=12.2, p=0.008), but there was no significant difference among treatments (two-way ANOVA: $F_{3,8}$=2.7, p=0.12). The total ^{13}C content of bacteria (mmol ^{13}C m^{-2}; Fig. 4a) did not change significantly with time, and was not significantly affected by treatment. The majority of the ^{13}C assimilated into the cores was present in the 0-2 cm depth (0-2 cm 2-5 cm 9 ± 0.8%; and 5-10 cm 5.2 ± 0.5% Supplemental Fig. 3a, b & c). ^{13}C incorporation was largely dominated by bacteria across all treatments in sediments below 2 cm, with few exceptions. Increased bacterial contribution

412 occurred more quickly and was more pronounced in nutrient amended treatments at both 2-5
413 cm and 5-10 cm (Supplemental Figs. 4 & 5).

414 Total uptake of excess ^{13}C (Fig. 4a), while informative about the amount of label
415 contained within each core at each time period, is not as useful for comparison between
416 microbial groups due to variations in the total amount of ^{13}C assimilated between cores. It is
417 important to consider the relative contribution to ^{13}C uptake (Fig. 4b) of both microbial groups
418 as each data point was sampled from separate cores that assimilated similar, but different,
419 initial concentrations of newly fixed ^{13}C. Significant MPB contribution (%) decreased for after
420 1.5 d (two-way ANOVA: $F_{1,8}$= 83.1, p<0.0001) but showed no difference between treatments
421 ($F_{3,8}$=8.2, p=0.008), although interaction between the variables was significant ($F_{3,8}$=8.2,
422 p=0.008). Tukey tests found that MPB contributed less to microbial uptake of ^{13}C in the
423 elevated treatment than in the ambient treatment (p=0.01) as well as the moderate treatment
424 being lower than the minimal treatment (p=0.014). MPB dominated the relative incorporation
425 of ^{13}C into microbial biomass at 0-2 cm in all treatments initially (0.5d; 90% ambient, 90%
426 minimal, 92% moderate, and 92% elevated; Fig. 4b) and throughout the 3.5 d incubation (81-
427 90% ambient, 82-91% minimal, 74-92% moderate, and 65-92% elevated; Fig. 4b). The
428 relative bacterial contribution to microbial ^{13}C incorporation increased across all treatments as
429 the incubations progressed, but increases in the moderate and elevated treatments at 2.5 and
430 3.5 d (Fig. 4b) corresponded with decreased ^{13}C incorporation into MPB (Fig. 4a).

431 **3.6.2 Uncharacterized**

432 A portion of the ^{13}C contained within sediment OC was uncharacterized, i.e., not
433 contained within the viable microbial biomass measured using PLFA biomarkers. Initially (0.5
434 d) the uncharacterized pool accounted for less sediment ^{13}C within the nutrient-amended

435 treatments (1-3%) than within the ambient treatment (12%; Fig. 3), indicating that there was
436 more ^{13}C contained in viable microbial biomass under increased nutrient availability after 12 h
437 of incubation. By 3.5 d increased contribution to the uncharacterized pool in the moderate and
438 elevated treatments (29% ambient, 32% minimal, 41% moderate and 45% elevated; Fig. 3)
439 corresponded with decreased ^{13}C contained in MPB (52% ambient, 49% minimal, 42%
440 moderate and 26% elevated). In contrast, changes in the ^{13}C in the uncharacterized pool did
441 not relate to ^{13}C contained in bacteria, as the bacterial contribution to ^{13}C remained relatively
442 unchanged (17% ambient, 14% minimal, 15% moderate and 15% elevated) and was similar
443 among treatments at 3.5 d.

444 **3.7 Loss of ^{13}C from sediment OC**

445 Rates of ^{13}C loss from sediment OC to the water column were highest in the moderate
446 and elevated treatments (total lost at 3.5 d: ambient 5%, minimal, 7%, moderate 11% and
447 elevated 20%; Fig. 5 & 6). Reflecting this, loss rate constants for the ^{13}C remaining in
448 sediment OC after accounting for losses of $DI^{13}C$ and $DO^{13}C$ across 3.5 d were equivalent for
449 ambient and minimal treatments (0.018 ± 0.024, $R^2 = 0.95$ and 0.021 ± 0.001, $R^2 = 0.99$,
450 respectively; Fig. 6), but were higher for both moderate and elevated treatments ($0.0383 \pm$
451 0.009, $R^2 = 0.86$, 0.0566 ± 0.003, $R^2 = 0.99$, respectively; Fig. 6).

452 Across all treatments, most of the ^{13}C loss from sediment during the incubation
453 occurred via DIC fluxes (Fig. 5). Cumulative ^{13}C export to the water column via DIC fluxes
454 was considerably larger than via DOC fluxes for all treatments (9× ambient, 11× minimal, 10×
455 moderate and 17× elevated). Initial $DI^{13}C$ loss (0.5 d) was higher in the elevated treatment
456 than in the ambient, minimal, and moderate treatments ($5.3 \pm 3.4\%$, versus 0%, $1.1 \pm 0.3\%$
457 and $1.4 \pm 1.4\%$, respectively; Fig. 5). After 3.5 d, cumulative losses of $DI^{13}C$ were higher in

moderate and elevated treatments (12.4 ± 11.6% moderate, 19.8 ± 10.8% elevated; Fig. 5) than in ambient (4.0 ± 3.2%) and minimal treatments (6.6 ± 2.0%; Fig. 5 & 7).

DOC export was a less important pathway for ^{13}C loss than DIC across all treatments. ^{13}C loss via DOC export was comparable and low across all treatments with similar maximum export at 3.5 d (0.5 ± 0.2% ambient, 0.5 ± 0.2% minimal, 0.4 ± 0.2% moderate, and 0.6 ± 0.5% elevated; Fig. 5).

4.0 Discussion

This study examined the effects of enhanced nutrient loading on the processing pathways for MPB-derived C in intertidal estuarine sediments. Enhanced nutrient availability 1) increased loss of MPB-derived C from sediment via DIC efflux (Fig. 5 & 6), 2) shifted benthic metabolism to be less autotrophic (Fig. 1), and 3) decreased retention of C within MPB (Fig. 3 & 4). These multiple lines of evidence indicate that intertidal sediments in areas experiencing increased nutrient loading are likely to process C differently, resulting in reduced potential for C retention within the sediment.

4.1 Loss pathways for ^{13}C

Increased nutrient additions caused additional loss of ^{13}C from sediment OC, largely driven by DIC fluxes to the water column (Fig. 5 & 6). Complete loss of newly produced C from sediment OC, as estimated from exponential decay functions, occurred more quickly in nutrient amended treatments than in ambient (15% increase minimal, 210% increase moderate and 310% increase elevated, Fig. 6). Increased loss rates indicated reduced turnover time for newly produced MPB-derived C under increased nutrient load (419 d ambient versus 199 d moderate and 134 d elevated). It should be noted that the loss rate constant for the minimal

Biogeosciences Discuss., https://doi.org/10.5194/bg-2017-448
Manuscript under review for journal Biogeosciences
Discussion started: 2 November 2017

480 treatment (0.021 ± 0.001, R^2 = 0.99, 366 d) was comparable to that for the ambient treatment
481 (0.018 ± 0.024, R^2 = 0.95, 419 d), indicating that a small nutrient addition may not cause
482 significant decreases in C turnover time. Increased loss rates imply that C retention and burial
483 in MPB-dominated photic sediments are greatest when nutrients are limiting and that
484 increased nutrient availability alters the processing of MPB-C within the sediment. Increased
485 nitrogen availability appears to have decreased the retention of C within MPB biomass (Fig.
486 3). Increased turnover of the newly fixed MPB-derived C from the sediment likely occurred as
487 the net result of exudation of material and breakdown of cells. This increased turnover may
488 have caused the increased efflux of MPB-derived C as exudates and cell components were
489 increasingly available to support respiration.

490 Across all treatments, DIC was the main loss pathway for MPB-C, DOC was a minor
491 pathway and loss via CO_2 was considered negligible (Oakes and Eyre 2014) (Fig. 5 & 6). Loss
492 of ^{13}C via the DIC pathway appears to be stimulated by nutrient additions, resulting in
493 increased export occurring earlier within incubations as a result of increased bacterial
494 remineralization (Fig. 2 & 5). Increased $DI^{13}C$ export represents the portion of $DI^{13}C$
495 produced via respiration in excess of that which is re-captured and utilized by MPB to drive
496 production. Given the close proximity of bacteria and MPB in the sediment, there is the
497 potential for considerable utilization of the $DI^{13}C$ arising from bacterial remineralization to
498 support algal production. Relatively low fluxes of $DI^{13}C$ to the water column in the ambient
499 treatment across 2.5 d likely indicate more complete utilization and recycling of $DI^{13}C$ to
500 support algal production (Fig. 5). Export of $DI^{13}C$ was considerably higher in both the
501 moderate and elevated treatments, indicating production of $DI^{13}C$ during bacterial
502 remineralization in excess of utilization of $DI^{13}C$ by MPB. Decreased recycling of $DI^{13}C$ from

remineralization in elevated treatments could develop due to 1) decreased DIC demand as algal production decreased after initial stimulation or 2) increased production of unlabeled DIC through remineralization of previously refractory organic material providing an alternative unlabeled source to support algal production.

Cumulative losses of $DO^{13}C$ were low for all treatments across 3.5 d (<1.5 % of total ^{13}C, Fig.5) and did not appear to change significantly with increased nutrient availability. Previous studies have also found that DOC fluxes are a relatively minor contributor to loss of MPB-derived carbon (Oakes et al. 2012; Oakes and Eyre 2014), as observed in the current study, but DOC may be a significant export pathway in other settings. Produced DOC may be labile and respired to DIC prior to loss from the sediment, but this pathway was not greatly altered in this study due to increased nutrient availability.

4.2 Shifts in benthic metabolism

Each nutrient amendment produced a different shift in benthic metabolism within the core incubations (Fig. 1) with no clear dose-effect relationship between increased nutrient availability and P/R observed among nutrient-amended treatments. Heterogeneity in both bacterial and MPB biomass are routinely observed within intertidal sediment and can lead to substantial variability between the production and respiration observed between cores (Eyre et al. 2005; Glud 2008). Despite a background of variability between cores, both minimal and elevated treatments display a decrease in autotrophy. The minimal treatment shifted into heterotrophy (P/R<1) and the elevated treatment stimulated initial algal production sufficient to cause a subsequent spike in respiration. Increased respiration by 3.5 d was partially offset by maintained production that kept P/R above 1. In contrast, the moderate treatment maintained a steady P/R across 3.5 d, although substantial error bars indicate considerable

526 variability between the cores within the treatment. Differences in the response among nutrient-
527 amended treatments appear to result from increased initial production that was supported in
528 both the elevated and moderate treatments, but that decreased by 3.5 d in the minimal
529 treatment. MPB-dominated sediment is expected to be net autotrophic, with positive GPP
530 (Tang and Kristensen 2007) that may be further stimulated by nutrient inputs (Underwood and
531 Kromkamp 1999). Increased algal production of labile organic matter subsequently stimulates
532 heterotrophic respiration, increasing oxygen consumption and lowering P/R (Glud 2008;
533 McGlathery et al. 2007). Quick increases in MPB productivity followed by increased
534 respiration have been observed in response to pulses of organic matter in both oligotrophic
535 and estuarine sediments (Eyre and Ferguson 2005; Glud et al. 2008). Rapid increases in
536 respiration rates, as reflected in the oxygen fluxes for the elevated treatment (Fig. 1a), are
537 often associated with an increased supply of labile C and can occur at rates higher than
538 expected for in situ temperature. This has been observed in subtropical sediments (Eyre and
539 Ferguson 2005) as well as polar and temperate systems (Banta et al. 1995; Rysgaard et al.
540 1998). Although the sediments in this study were not oligotrophic, the extent of the shift
541 towards heterotrophy is still likely controlled by the amount and relative quality (C/N ratio) of
542 the organic matter available for processing (Cook et al. 2009; Eyre et al. 2008). The similarity
543 in initial P/R ratios between ambient and minimal treatments indicate that a small nutrient
544 addition did not stimulate large increases in algal production, but rather a small increase in
545 production that was offset by increased respiration in the minimal treatment (Fig. 1). The
546 moderate treatment had a distinctly different reaction to increased nutrient availability, with
547 stable P/R as both production and respiration were maintained across 3.5 d. The elevated
548 treatment had increased algal production at 1.5 d, with the highest production rate observed in

549 this study, and this was followed by a considerable increase in respiration by 3.5 d (increased
550 dark uptake of O_2; Fig. 1). Decreased autotrophy by 3.5 d was a result of both elevated
551 respiration driven by increased bacterial decomposition of labile material and declining MPB
552 production. It is important to note that the elevated treatment did not shift to a P/R less than 1,
553 but did display a considerable increase in respiration. The rapid increase in respiration in the
554 elevated treatment suggests that the newly produced organic matter was readily bioavailable
555 and quickly processed by bacteria as a result of increased nutrient availability.

556 **4.3 Retention of carbon within microphytobenthos biomass**

557 Within surface sediments, MPB biomass did not increase with increased nutrient load,
558 despite apparent increases in productivity (Supplemental Fig. 2). Although MPB biomass did
559 not change, by 3.5 d the ^{13}C retained within MPB biomass in the nutrient-amended treatments
560 appears to have decreased (Fig. 4a) indicating increased turnover of newly fixed C out of
561 MPB biomass. This aligns with many previous reports that increased productivity does not
562 necessarily correspond with increased algal biomass (Alsterberg et al. 2012; Ferguson and
563 Eyre 2013; Ferguson et al. 2007; Hillebrand and Kahlert 2002; Piehler et al. 2010; Spivak and
564 Ossolinski 2016). Lack of change in MPB biomass, despite increased productivity, may occur
565 as a result of grazing or secondary nutrient limitation (Hillebrand and Kahlert 2002), but these
566 explanations are unlikely for the current study. Grazing is likely to have occurred at only a
567 low level. There was very little fauna, including grazers, within sediment at the study site and,
568 although any grazers such as copepods that were within the site water would have been
569 included in the incubations, larger, mobile grazers were excluded. Secondary nutrient
570 limitation of P or Si was avoided through additions of both elements at 0 d for P and 2.5 d for
571 Si during incubation. It is more likely that the microbial community responded to pulses of

Biogeosciences Discuss., https://doi.org/10.5194/bg-2017-448
Manuscript under review for journal Biogeosciences
Discussion started: 2 November 2017

572 increased nutrients through increased production of extracellular compounds (MPB:
573 carbohydrates; bacteria: enzymes) rather than increasing their biomass (Thornton et al. 2010).
574 This may be a strategy to optimally utilize intermittently available nutrient resources, given
575 that increased cell numbers (biomass) within a biofilm community may otherwise increase
576 competition among cells (Decho 2000; Drescher et al. 2014). Allocation of additional N
577 towards increased production of extracellular enzymes or storage molecules rather than new
578 biomass may therefore benefit the community. Strong competition between MPB and bacteria
579 for available N resulted in a minimal contribution from denitrification as a pathway for N loss
580 likely as a result of limited availability of NO_3^- for denitrifying bacteria (unpubl. data).

581 **4.4 ^{13}C distribution within the sediment**

582 **4.4.1 Microbial biomass**

583 Decreased autotrophy is somewhat reflected in the relative partitioning of ^{13}C from
584 newly produced algal C between MPB and bacteria within the individual treatments (Fig. 1 &
585 Fig. 4b). Initially, uptake of ^{13}C was strongly dominated by MPB amongst treatments, with
586 minimal incorporation by bacteria. As incubations progressed, a shift towards increased
587 relative contribution by bacteria was apparent in all treatments, but was more substantial in the
588 elevated treatment (3.5 d; 19% ambient, 18% minimal, 26% moderate, and 35% elevated, Fig.
589 4b). This quicker shift towards bacterial dominance of ^{13}C incorporation corresponded with
590 the largest decrease in P/R ratios observed in this study, as increased respiration and decreased
591 production caused the elevated treatment to become less autotrophic (Fig. 1). These
592 corresponding factors are likely a result of a tight coupling and intense recycling between
593 algal production and bacterial processing of newly produced MPB-derived C. EPS can be a
594 large export pathway for newly fixed C from algal cells (up to 70.3% Goto et al. 1999) and

595 can provide a labile C source for heterotrophic or denitrifying bacteria. The ^{13}C incorporated
596 into bacteria represents the balance of respiration and uptake and is expected to become
597 increasingly muddled by ^{13}C being processed through other pathways (denitrification) as
598 incubations progress. Therefore, this study only considered the transfer of MPB-C into
599 bacteria at the 0.5 d sampling. However, given the low initial transfer of ^{13}C to bacteria in all
600 treatments over 24 h following labeling (0.5 d; 0.8% h^{-1} ambient, 0.8% h^{-1} minimal, 0.7% h^{-1}
601 moderate, 0.7% h^{-1} elevated; Fig. 3) it appears that either production or utilization of EPS
602 containing newly fixed C was relatively low in the current study, regardless of nutrient
603 addition. This transfer was the net result of EPS production and bacterial remineralization and
604 would have become increasingly muddled as ^{13}C-containing detrital material accumulated as
605 incubations progressed. Low EPS production at 0.5 d may indicate that N is not limiting for
606 MPB in these sediments, as exuded EPS does not appear to be copious, as would be expected
607 under severe N limitation (van Den Meersche et al. 2004). Similarly low rates of C transfer
608 from MPB to bacteria were previously reported for the site (0.83% h^{-1}, Oakes and Eyre 2014)
609 and are towards the lower end of the range of EPS production rates for benthic diatoms (0.05
610 to 73% h^{-1}; Underwood and Paterson 2003). At 0.5 d nutrient availability appears to have had
611 little effect on the initial transfer rates from MPB to bacteria, but appears to have decreased
612 the turnover of MPB-C out of the microbial community, as contributions of ^{13}C to the
613 uncharacterized pool were lower in the nutrient-amended treatments (Fig. 3). By 3.5 d,
614 increased nutrient availability appears to stimulate the transfer of ^{13}C from microbial biomass
615 in the uncharacterized pool, but had no effect on ^{13}C in bacteria as the bacterial pool was equal
616 across all treatments (15-18%, Fig. 3 & 7).

617

Biogeosciences Discuss., https://doi.org/10.5194/bg-2017-448
Manuscript under review for journal Biogeosciences
Discussion started: 2 November 2017

618 **4.4.2 Uncharacterized**

619 A portion of the ^{13}C incorporated into sediment OC was uncharacterized (i.e., not
620 within microbial biomass). By 3.5 d, the portion of initially incorporated ^{13}C that was within
621 the uncharacterized pool varied substantially among the treatments (29-46%, Fig. 7). This
622 uncharacterized C is likely to represent a mixture of both labile and refractory OC (Veuger et
623 al. 2012), including metabolic byproducts, senescent cells undergoing breakdown, EPS,
624 extracellular enzymes, carbohydrates, and a variety of complex, molecularly uncharacterized
625 organic matter (Hedges et al. 2000). Collectively, these molecules form a pool of labeled intra
626 and extra-cellular material remaining in sediment OC derived from both MPB and bacteria
627 that is not characterized as microbial biomass when using PLFAs to estimate microbial
628 biomass (e.g., ^{13}C contained in storage products or enzymes that was not incorporated into
629 phospholipids). Given that MPB can direct up to 70% of their newly fixed C to EPS (Goto et
630 al. 1999), carbohydrates are likely to form a considerable portion of the uncharacterized ^{13}C.
631 A study using a similar ^{13}C-labeling approach reported that 15-30% of MPB-derived carbon
632 was transferred to intra- and extracellular carbohydrates within 30 d after an initial transfer
633 rate of ~0.4% into bacteria (2 d; Oakes et al. 2010a). In light of the higher transfer rates for
634 ^{13}C into bacteria observed in this study (0.7 to 0.9% h^{-1}), there is potential for a considerable
635 portion of the uncharacterized pool to be accounted for by EPS.

636 When quantified, the uncharacterized C pool typically has a high C:N ratio (10 to 60;
637 Cook et al. 2009; Eyre et al. 2016a), indicating that nitrogen availability may have a role in
638 regulating its content and accumulation. Given that nitrogen limitation has been observed to
639 suppress processing pathways of otherwise labile OM in soils (Jian et al. 2016; Schimel and
640 Bennett 2004), a similar mechanism may be possible in estuarine sediments. This mechanism

641 may include a priming effect due to either increased production of extracellular enzymes or
642 due to increased energy from labile C compounds allowing for the increased breakdown of
643 sediment OM (Bianchi 2011). Increased extracellular enzyme production would result in more
644 complete utilization of sediment OM through promotion of hydrolysis (Arnosti 2011; Huettel
645 et al. 2014), a potentially limiting step during the breakdown of organic material. This would
646 result in more complete utilization of ^{13}C by microbial biomass and a smaller pool of
647 uncharacterized C within sediment OC, as was observed in the nutrient-amended treatments at
648 0.5 d (Fig. 3). This is further supported by the increased turnover of MPB-C from microbial
649 biomass into the uncharacterized pool observed within the nutrient amended treatments (2.5 d,
650 Fig. 3) indicating ^{13}C that was previously incorporated into MPB was processed into the
651 uncharacterized pool more quickly with increased nutrient availability. After 2.5 d, the ^{13}C
652 content of the uncharacterized pool was substantially larger for the elevated treatment (Fig. 3
653 & 7) and looks to have been largely sourced from MPB ^{13}C, given that bacterial contribution
654 to sediment OM remained stable. Composition of the uncharacterized pool will be study-
655 specific depending on the different biomarker techniques utilized to estimate microbial
656 biomass incorporating different pools of material. The metabolic pathways and ecological
657 strategies regulating the portion of ^{13}C entering the uncharacterized pool warrant further
658 investigation.

659 **4.5 Downward transport**

660 Increased nutrient availability reduced the downward transport of fixed ^{13}C,
661 particularly within 2-5 cm, mainly as a result of increased export of MPB-C to the water
662 column. In the ambient treatment, downward transport to 2-5 cm (10.0%) and 5-10 cm (9.2%)
663 across 60 h was comparable to that reported by Oakes and Eyre (2014) for the same site (8.3%

2-5 cm, 14.9% 5-10 cm, 60 h). Oakes and Eyre (2014) suggested that resuspension resulting from a flood event limited the downward transport of ^{13}C, but a comparable and lower rate of downward transport at 60 h (12.1% 2-5 cm, 9% 5-10 cm, ambient treatment) was observed in the current study in the absence of marked freshwater inflow. Downward transport is not a large pathway for loss of ^{13}C within this system as transport to sediment below 2 cm was minimal, and appeared further reduced in the elevated treatment (Supplemental Fig. 3b & c). Decreased downward transport of MPB-derived C under increased nutrient load may reflect 1) decreased transport to depth as diatoms reduce migration downward to find nutrients (Saburova and Polikarpov 2003) or 2) relaxation of the tight recycling and retention of newly fixed C between MPB and bacteria within surface sediments allowing for increased export of labile C to the water column (Cook et al. 2007). Decreased downward transport in this study likely reflects a combination of reduced algal transport of ^{13}C to depth and increased loss of ^{13}C from surface sediments to the water column.

4.6 Implications

This study has provided valuable insight into the processing of MPB-derived C under increased nutrient availability using multiple lines of evidence (budgeting ^{13}C within sediment compartments and sediment-water effluxes, partitioning of C pools via biomarkers, and changes in P/R) and is among the first to have addressed this problem. However, some caveats on interpretation are important to note, as follows: 1) *Ex situ* incubation of sediment cores may not be directly comparable to processes occurring *in situ* and may overestimate C retention, as there is reduced potential for loss via sediment resuspension due to tidal movement, water currents, and grazing. 2) Removal of grazers may also increase MPB production and their release of exudates (Fouilland et al. 2014), which could enhance ^{13}C

687 transfer to bacteria. However, given the lack of apparent grazers at the site of the current
688 study, and the low observed ^{13}C transfer rate to bacteria (0.7-0.9% h^{-1} Fig. 4b) that was
689 comparable to previously measured in situ rates in Oakes and Eyre (2014), grazers appear to
690 have had little potential impact on sediment processing in this study.

691 The findings show that increased nutrient availability reduced C retention, but the
692 main export pathway for algal carbon remained the same (primarily loss via DIC). Coastal
693 environments are recognized as important sites for carbon storage. Although the focus has
694 primarily been on vegetated environments (Duarte et al. 2005), which store the most carbon,
695 unvegetated sediments also have capacity for longer-term retention (e.g. 30% after 30 d Oakes
696 and Eyre 2014; 31% after 30 d Oakes et al. 2012). Based on N burial rates (and corresponding
697 unpublished C burial rates) some coastal systems can have higher C burial rates in subtidal
698 and intertidal macrophyte-free MPB sediments than in macrophyte-dominated sediments
699 (Eyre et al. 2016b; Maher and Eyre 2011) although this was shown in only one of the three
700 estuaries studied. Increased nutrient loading into coastal settings has been implicated in
701 historical decreases of long-term carbon storage through a shift from macrophyte dominated
702 systems (seagrass and mangrove) towards MPB dominated systems (Macreadie et al. 2012)
703 within coastal environments. Carbon storage potential within MPB dominated sediments
704 remains a significant knowledge gap within the carbon budgets of estuaries. At 30 d, estimates
705 of retention of C identified for ambient and minimal treatments were considerable in the
706 current study (58% and 54%), however, increased nutrient loading reduced this retention
707 considerably (32% moderate, 18% elevated). Given that nutrient inputs have increased
708 globally and bare photic sediment accounts for a large surface area within estuaries, these two
709 factors could have resulted in substantial release of currently stored carbon and demonstrate

the capacity for further substantial reduction of C storage potential globally if elevated nutrient inputs continue within estuarine systems.

Although MPB-dominated sediments probably have less decadal-scale long-term storage of C than macrophyte-dominated sediments, this study clearly demonstrates that the existing storage potential is further degraded by increased nutrient loading within MPB-dominated sediments. These sediments may lock away less C per area, but are fairly ubiquitous within photic coastal and oceanic sediment and may contribute significantly to carbon storage within coastal systems due to this increased area. The observed increases in mobility of newly fixed algal carbon from intertidal sediments (Fig. 5) as a result of elevated anthropogenic nutrient loading will directly translate to increased carbon export to coastal oceans and reduced carbon storage potential within shallow photic estuarine sediments.

References

Alsterberg, C., K. Sundback, and S. Hulth. 2012. Functioning of a shallow-water sediment system during experimental warming and nutrient enrichment. Plos One **7:** 10.

Andersson, J. H. and others 2008. Short-term fate of phytodetritus in sediments across the Arabian Sea Oxygen Minimum Zone. Biogeosciences **5:** 43-53.

Armitage, A. R., and P. Fong. 2004. Upward cascading effects of nutrients: shifts in a benthic microalgal community and a negative herbivore response. Oecologia **139:** 560-567.

Arnosti, C. 2011. Microbial extracellular enzymes and the marine carbon cycle. Ann. Rev. Mar. Sci. **3:** 401-425.

Banta, G. T., A. E. Giblin, J. E. Hobbie, and J. Tucker. 1995. Benthic respiration and nitrogen release in Buzzards Bay, Massachusetts. J. Mar. Res. **53:** 107-135.

Bauer, J. E., W. J. Cai, P. A. Raymond, T. S. Bianchi, C. S. Hopkinson, and P. G. Regnier. 2013. The changing carbon cycle of the coastal ocean. Nature **504:** 61-70.

734 Bellinger, B. J., G. J. C. Underwood, S. E. Ziegler, and M. R. Gretz. 2009. Significance of
735 diatom-derived polymers in carbon flow dynamics within estuarine biofilms
736 determined through isotopic enrichment. Aquat. Microb. Ecol. **55:** 169-187.
737 Bianchi, T. S. 2011. The role of terrestrially derived organic carbon in the coastal ocean: A
738 changing paradigm and the priming effect. P. Natl. Acad. Sci. **108:** 19473-19481.
739 Brinch-Iversen, J., and G. M. King. 1990. Effects of substrate concentration, growth state, and
740 oxygen availability on relationships among bacterial carbon, nitrogen and
741 phospholipid content. FEMS Microb. Ecol. **74:** 345-356.
742 Cook, P., D. Van Oevelen, K. Soetaert, and J. Middelburg. 2009. Carbon and nitrogen cycling
743 on intertidal mudflats of a temperate Australian estuary. IV. Inverse model analysis
744 and synthesis. Mar. Ecol. Prog. Ser. **394:** 35-48.
745 Cook, P. L. M., B. Veuger, S. Boer, and J. J. Middelburg. 2007. Effect of nutrient availability
746 on carbon and nitrogen and flows through benthic algae and bacteria in near-shore
747 sandy sediment. Aquat. Microb. Ecol. **49:** 165-180.
748 Decho, A. W. 2000. Microbial biofilms in intertidal systems: an overview. Cont. Shelf Res.
749 **20:** 1257-1273.
750 Drenovsky, R. E., G. N. Elliott, K. J. Graham, and K. M. Scow. 2004. Comparison of
751 phospholipid fatty acid (PLFA) and total soil fatty acid methyl esters (TSFAME) for
752 characterizing soil microbial communities. Soil Biol. Biochem. **36:** 1793-1800.
753 Drescher, K., Carey d. Nadell, Howard a. Stone, Ned s. Wingreen, and Bonnie l. Bassler.
754 2014. Solutions to the public goods dilemma in bacterial biofilms. Curr. Biol. **24:** 50-
755 55.
756 Duarte, C. M., J. J. Middelburg, and N. Caraco. 2005. Major role of marine vegetation on the
757 oceanic carbon cycle. Biogeosciences **2:** 1-8.
758 Edlund, A., P. D. Nichols, R. Roffey, and D. C. White. 1985. Extractable and
759 lipopolysaccharide fatty acid and hydroxy acid profiles from *Desulfovibrio* species. J.
760 Lipid Res. **26:** 982-988.
761 Evrard, V., M. Huettel, P. L. M. Cook, K. Soetaert, C. H. R. Heip, and J. J. Middelburg. 2012.
762 Importance of phytodetritus and microphytobenthos for heterotrophs in a shallow
763 subtidal sandy sediment. Mar. Ecol. Prog. Ser. **455:** 13-31.

764 Eyre, B. 1997. Water quality changes in an episodically flushed sub-tropical Australian
765 estuary: A 50 year perspective. Mar. Chem. **59:** 177-187.
766 Eyre, B., R. N. Glud, and N. Patten. 2008. Mass coral spawning: A natural large-scale nutrient
767 addition experiment. Limnology and Oceanography **53:** 997-1013.
768 Eyre, B., J. M. Oakes, and J. J. Middelburg. 2016a. Fate of microphytobenthos nitrogen in
769 subtropical sediments: A ^{15}N pulse-chase study. Limnol. Oceanogr. **61:** 1144-156.
770 Eyre, B. D. 2000. Regional evaluation of nutrient transformation and phytoplankton growth in
771 nine river-dominated sub-tropical east Australian estuaries. Mar. Ecol. Progr. Ser. **205:**
772 61-83.
773 Eyre, B. D., and A. J. P. Ferguson. 2005. Benthic Metabolism and Nitrogen Cycling in a
774 Subtropical East Australian Estuary (Brunswick): Temporal Variability and
775 Controlling Factors. Limnol. Oceanogr. **50:** 81-96.
776 Eyre, B. D., A. J. P. Ferguson, A. Webb, D. Maher, and J. M. Oakes. 2011. Metabolism of
777 different benthic habitats and their contribution to the carbon budget of a shallow
778 oligotrophic sub-tropical coastal system (southern Moreton Bay, Australia).
779 Biogeochemistry **102:** 87-110.
780 Eyre, B. D., D. T. Maher, and C. Sanders. 2016b. The contribution of denitrification and
781 burial to the nitrogen budgets of three geomorphically distinct Australian estuaries:
782 Importance of seagrass habitats. Limnol. Oceanogr. **61:** 1144-1156.
783 Ferguson, A., and B. Eyre. 2013. Interaction of benthic microalgae and macrofauna in the
784 control of benthic metabolism, nutrient fluxes and denitrification in a shallow sub-
785 tropical coastal embayment (western Moreton Bay, Australia). Biogeochemistry **112:**
786 423-440.
787 Ferguson, A., B. Eyre, J. Gay, N. Emtage, and L. Brooks. 2007. Benthic metabolism and
788 nitrogen cycling in a sub-tropical coastal embayment: spatial and seasonal variation
789 and controlling factors. Aquat. Microb. Ecol. **48:** 175-195.
790 Ferguson, A., B. Eyre, and J. Gay. 2003. Organic matter and benthic metabolism in euphotic
791 sediments along shallow sub-tropical estuaries, northern New South Wales, Australia.
792 Aquat. Microb. Ecol. **33:** 137-154.

793 Ferguson, A., B. Eyre, and J. Gay. 2004. Benthic nutrient fluxes in euphotic sediments along
794 shallow sub-tropical estuaries, northern New South Wales, Australia. Aquat. Microb.
795 Ecol. **37:** 219-235.
796 Fouilland, E. and others 2014. Bacterial carbon dependence on freshly produced
797 phytoplankton exudates under different nutrient availability and grazing pressure
798 conditions in coastal marine waters. FEMS Microb. Ecol. **87:** 757-769.
799 Fry, B. and others 2015. Carbon dynamics on the Louisiana continental shelf and cross-shelf
800 feeding of hypoxia. Estuar Coast **38:** 703-721.
801 Glud, R. N. 2008. Oxygen dynamics of marine sediments. Marine Biology Research **4:** 243-
802 289.
803 Glud, R. N., B. D. Eyre, and N. Patten. 2008. Biogeochemical responses to mass coral
804 spawning at the Great Barrier Reef: Effects on respiration and primary production.
805 Limnol. Oceanogr. **53:** 1014-1024.
806 Goto, N., T. Kawamura, O. Mitamura, and H. Terai. 1999. Importance of extracellular organic
807 carbon production in the total primary production by tidal-flat diatoms in comparison
808 to phytoplankton. Mar. Ecol. Prog. Ser. **190:** 289-295.
809 Hardison, A., I. Anderson, E. Canuel, C. Tobias, and B. Veuger. 2011. Carbon and nitrogen
810 dynamics in shallow photic systems: Interactions between macroalgae, microalgae,
811 and bacteria. Limnol. Oceanogr. **56:** 1489-1503.
812 Hardison, A., E. Canuel, I. Anderson, C. Tobias, B. Veuger, and M. Waters. 2013.
813 Microphytobenthos and benthic macroalgae determine sediment organic matter
814 composition in shallow photic sediments. Biogeosciences **10:** 2791-2834.
815 Hedges, J. I. and others 2000. The molecularly-uncharacterized component of nonliving
816 organic matter in natural environments. Org. Geochem. **31:** 945-958.
817 Hillebrand, H., and M. Kahlert. 2002. Effect of grazing and water column nutrient supply on
818 biomass and nutrient content of sediment microalgae. Aquat. Bot. **72:** 143-159.
819 Huettel, M., P. Berg, and J. Kostka. 2014. Benthic Exchange and Biogeochemical Cycling in
820 Permeable Sediments. Ann. Rev. Mar. Sci. **6:** 23-51.
821 Jian, S. and others 2016. Soil extracellular enzyme activities, soil carbon and nitrogen storage
822 under nitrogen fertilization: A meta-analysis. Soil Biol. Biochem. **101:** 32-43.

Lorenzen, C. 1967. Determinations of chlorophyll and phaeopigments: spectrophotometric equations. Limnol. Oceanogr. **12:** 343-346.

Macreadie, P. I., K. Allen, B. P. Kelaher, P. J. Ralph, and C. G. Skilbeck. 2012. Paleoreconstruction of estuarine sediments reveal human-induced weakening of coastal carbon sinks. Glob. Change Biol. **18:** 891-901.

Maher, D., and B. D. Eyre. 2011. Benthic carbon metabolism in southeast Australian estuaries: Habitat importance, driving forces, and application of artificial neural network models. Mar. Ecol. Prog. Ser. **439:** 97-115.

McGlathery, K. J., K. Sundbäck, and I. C. Anderson. 2007. Eutrophication in shallow coastal bays and lagoons: The role of plants in the coastal filter. Mar. Ecol. Prog. Ser. **348:** 1-18.

McKee, L. J., B. D. Eyre, and S. Hossain. 2000. Transport and retention of nitrogen and phosphorus in the sub-tropical Richmond River estuary, Australia: A budget approach. Biogeochemistry **50:** 241-278.

Middelburg, J. J., C. Barranguet, H. T. S. Boschker, M. J. Herman, T. Moens, and C. Heip. 2000. The fate of intertidal microphytobenthos carbon: An in situ ^{13}C-labeling study. Limnol. Oceanogr. **45:** 1224-1225.

Miyatake, T., T. C. W. Moerdijk-Poortvliet, L. J. Stal, and H. T. S. Boschker. 2014. Tracing carbon flow from microphytobenthos to major bacterial groups in an intertidal marine sediment by using an in situ ^{13}C pulse-chase method. Limnol. Oceanogr. **59:** 1275-1287.

Nordström, M. C., C. A. Currin, T. S. Talley, C. R. Whitcraft, and L. A. Levin. 2014. Benthic food-web succession in a developing salt marsh. Mar. Ecol. Prog. Ser. **500:** 43-55.

Oakes, J., B. Eyre, D., J. J. Middelburg, and H. T. S. Boschker. 2010a. Composition, production, and loss of carbohydrates in subtropical shallow subtidal sandy sediments: Rapid processing and long-term retention revealed by ^{13}C-labeling. Limnol. Oceanogr. **55:** 2126-2138.

Oakes, J. M., B. Eyre, D., and J. J. Middelburg. 2012. Transformation and fate of microphytobentos carbon in subtropical shallow subtidal sands: A ^{13}C-labeling study. Limnol. Oceanogr. **57:** 1846-1856.

853 Oakes, J. M., and B. D. Eyre. 2014. Transformation and fate of microphytobenthos carbon in
854 subtropical, intertidal sediments: Potential for long-term carbon retention revealed by
855 ^{13}C-labeling. Biogeosciences **11:** 1927-1940.
856 Oakes, J. M., B. D. Eyre, D. J. Ross, and S. D. Turner. 2010b. Stable isotopes trace estuarine
857 transformations of carbon and nitrogen from primary- and secondary-treated paper and
858 pulp mill effluent. Environ. Sci. Technol. **44:** 7411-7417.
859 Oakes, J. M., S. Rysgaard, R. N. Glud, and B. D. Eyre. 2016. The transformation and fate of
860 sub-Arctic microphytobenthos carbon revealed through ^{13}C-labeling. Limnol.
861 Oceanogr. **61:** 2296-2308.
862 Piehler, M. F., C. A. Currin, and N. S. Hall. 2010. Estuarine intertidal sandflat benthic
863 microalgal responses to in situ and mesocosm nitrogen additions. J. Exp. Mar. Biol.
864 Ecol. **390:** 99-105.
865 Rajendran, N., O. Matsuda, Y. Urushigawa, and U. Simidu. 1994. Characterization of
866 microbial community structure in the surface sediment of Osaka Bay, Japan, by
867 phospholipid fatty acid analysis. Appl. Environ. Microb. **60:** 248-257.
868 Rajendran, N., Y. Suwa, and Y. Urushigawa. 1993. Distribution of phospholipid ester-linked
869 fatty acid biomarkers for bacteria in the sediment of Ise Bay, Japan. Mar. Chem. **42:**
870 39-56.
871 Riekenberg, P. M., J. M. Oakes, and B. D. Eyre, 2017. Uptake of dissolved organic and
872 inorganic nitrogen in microalgae-dominated sediment: Comparing dark and light *in*
873 *situ* and *ex situ* additions of ^{15}N. Mar. Ecol. Prog. Ser. **571:** 29-42.
874 Rysgaard, S. and others 1998. Seasonal carbon and nutrient mineralization in a high-Arctic
875 coastal marine sediment, Young Sound, Northeast Greenland. Mar. Ecol. Prog. Ser.
876 **175:** 261-276.
877 Saburova, M. A. , and I. G. Polikarpov. 2003. Diatom activity within soft sediments:
878 behavioural and physiological processes. Mar. Ecol. Prog. Ser. **251:** 115-126.
879 Schimel, J. P., and J. Bennett. 2004. Nitrogen mineralization: Challenges of a changing
880 paradigm. Ecology **85:** 591-602.
881 Spivak, A. C. 2015. Benthic biogeochemical responses to changing estuary trophic state and
882 nutrient availability: A paired field and mesocosm experiment approach. Limnol.
883 Oceanogr. **60:** 3-21.

884 Spivak, A. C., and J. Ossolinski. 2016. Limited effects of nutrient enrichment on bacterial
885 carbon sources in salt marsh tidal creek sediments. Mar. Ecol. Prog. Ser. **544:** 107-130.
886 Stal, L. J. 2010. Microphytobenthos as a biogeomorphological force in intertidal sediment
887 stabilization. Ecol. Eng. **36:** 236-245.
888 Tang, M., and E. Kristensen. 2007. Impact of microphytobenthos and macroinfauna on
889 temporal variation of benthic metabolism in shallow coastal sediments. J. Exp. Mar.
890 Biol. Ecol. **349:** 99-112.
891 Thornton, D.C.O., S.M. Kopac, and R.A. Long. 2010. Production and enzymatic hydrolysis of
892 carbohydrates in intertidal sediment. Aquat. Microb. Ecol. **60:** 109-125.
893 Underwood, G. J. C., and J. Kromkamp. 1999. Primary production by phytoplankton and
894 microphytobenthos in estuaries, p. 93-153. Advances in Ecological Research.
895 Underwood, G. J. C., and D. M. Paterson. 2003. The importance of extracellular carbohydrate
896 production by marine epipelic diatoms, p. 183-240. Advances in Botanical Research.
897 Academic Press.
898 Van Nugteren, P., L. Moodley, G.-J. Brummer, C. H. R. Heip, P. M. J. Herman, and J. J.
899 Middelburg. 2009. Seafloor ecosystem functioning: the importance of organic matter
900 priming. Mar. Biol. **156:** 2277-2287.
901 Van Oevelen, D., J. J. Middelburg, K. Soetaert, and L. Moodley. 2006. The fate of bacterial
902 carbon in an intertidal sediment: Modeling an in situ isotope tracer experiment.
903 Limnol. Oceanogr. **51:** 1302-1314.
904 Veuger, B., D. Van Oevelen, and J. J. Middelburg. 2012. Fate of microbial nitrogen, carbon,
905 hydrolysable amino acids, monosaccharides, and fatty acids in sediment. Geochim.
906 Cosmochim. Acta **83:** 217-233.
907 Volkman, J. K., S. W. Jeffrey, P. D. Nichols, G. I. Rogers, and C. D. Garland. 1989. Fatty acid
908 and lipid composition of 10 species of microalgae used in mariculture. J. Exp. Mar.
909 Biol. Ecol. **128:** 219-240.

910 **Author Contribution**

911 PR planned the experimental design and field work, performed the field work, isolation of
912 biomarkers and laboratory analysis, and wrote the manuscript. JO planned the experimental

913 design and field work, contributed to the data interpretation and assisted with statistical
914 analysis and writing of the manuscript. BE planned the experimental design and field work,
915 contributed to the data interpretation and assisted with the writing of the manuscript. The
916 group of co-authors has approved the submission of this manuscript.

917 **Acknowledgements**

918 We thank Natasha Carlson-Perret and Jessica Riekenberg for field assistance, Iain
919 Alexander for laboratory analysis, and Matheus Carvalho for isotope analysis. This study was
920 funded by an Australian Research Council (ARC) Linkage Infrastructure, Equipment and
921 Facilities grant to B.D.E. (LE0668495), an ARC Discovery Early Career Researcher Award to
922 J.M.O. (DE120101290), an ARC Discovery grant to B.D.E. (DP160100248), and ARC
923 Linkage Grants to B.D.E. (LP110200975; LP150100451; LP150100519).

924

Biogeosciences Discuss., https://doi.org/10.5194/bg-2017-448
Manuscript under review for journal Biogeosciences
Discussion started: 2 November 2017

925 **Figures and Tables**

926

		Top Scrape				0 to 2 cm				2 to 5 cm				5 to 10 cm			
		Biomass	SE	$\delta^{13}C$	SE	Biomass	SE	$\delta^{13}C$	SE	Biomass	SE	$\delta^{13}C$	SE	Biomass	SE	$\delta^{13}C$	SE
Control cores	Sediment organic carbon	318.0	32.3	-18.7	0.3	3818.0	804.2	-20.7	0.3	7963.3	1174.9	-22.0	0.4	8498.2	1165.2	-22.1	0.4
	Microphytobenthos biomass					321.9	42.0			226.2	33.1			227.3	37.3		
	Bacterial biomass					500.4	65.3			286.0	68.8			244.1	66.1		
Initial cores	Sediment organic carbon	376.4	4.5	121.4	23.7	3693.6	382.4	-7.5	2.1	5056.8	117.8	-19.4	1.0	8397.0	492.5	-21.4	0.7

927 **Table 1:** $\delta^{13}C$ values (‰) and carbon biomass (µmol C m^{-2}) for control (natural abundance,
928 n=3) and initially labeled cores (n=3, 0 d). Microphytobenthos and bacterial biomass are only
929 provided for control cores.

Biogeosciences Discuss., https://doi.org/10.5194/bg-2017-448
Manuscript under review for journal Biogeosciences
Discussion started: 2 November 2017

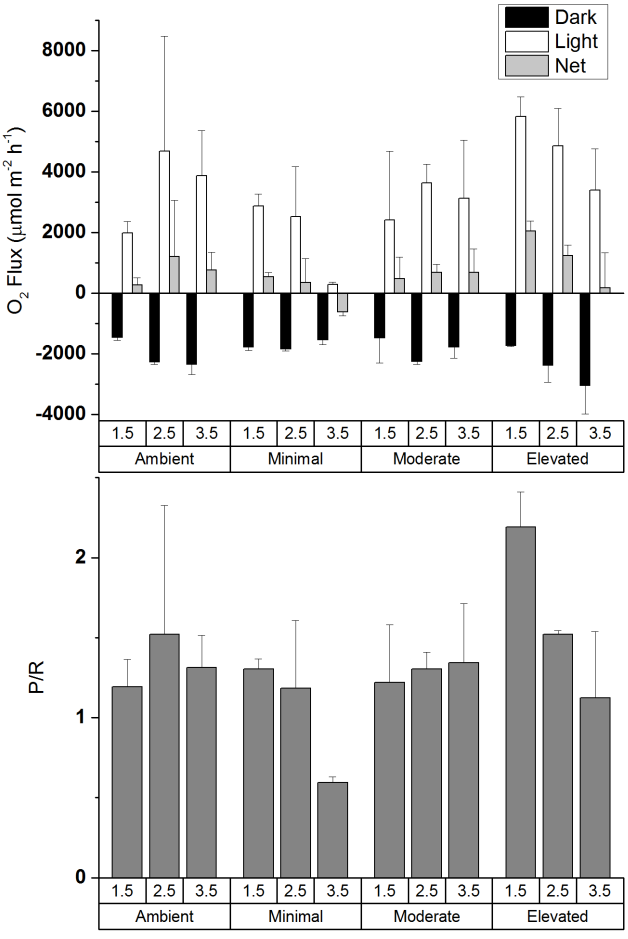

930

931 **Figure 1:** Oxygen fluxes and ratio of production to respiration (P/R) for all treatments across

932 24 h calculated from oxygen fluxes for individual cores. Values are mean ± SE.

Biogeosciences Discuss., https://doi.org/10.5194/bg-2017-448
Manuscript under review for journal Biogeosciences
Discussion started: 2 November 2017

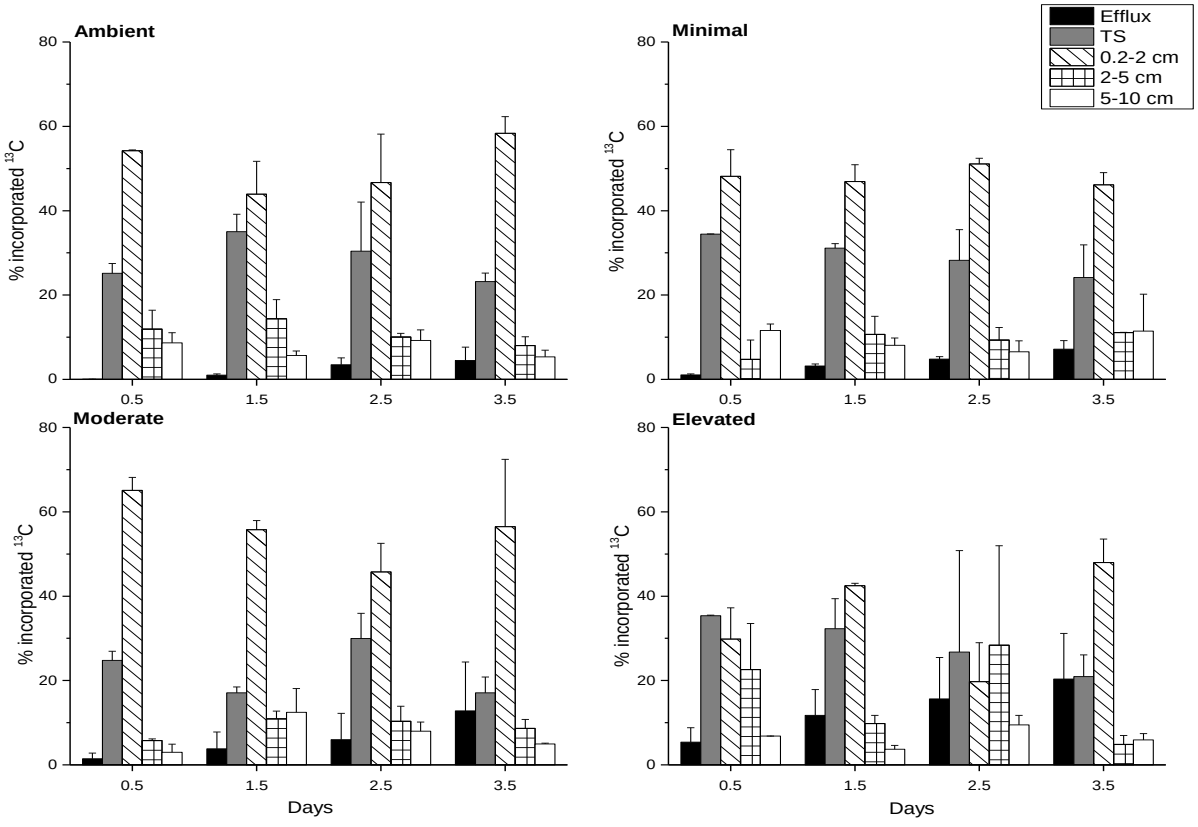

933

934 **Figure 2:** Carbon budget for excess ^{13}C within sediment OC at top scrape (TS), 0.2 to 2 cm, 2
935 to 5 cm, 5-10 cm, and the cumulative excess ^{13}C exported to the water column via the
936 combined efflux of DIC and DOC for each treatment at each sampling time. All values are as
937 a percentage of the ^{13}C initially incorporated into sediment OC (0-10 cm). Some error bars are
938 too small to be seen (mean ± SE).

939

Biogeosciences Discuss., https://doi.org/10.5194/bg-2017-448
Manuscript under review for journal Biogeosciences
Discussion started: 2 November 2017

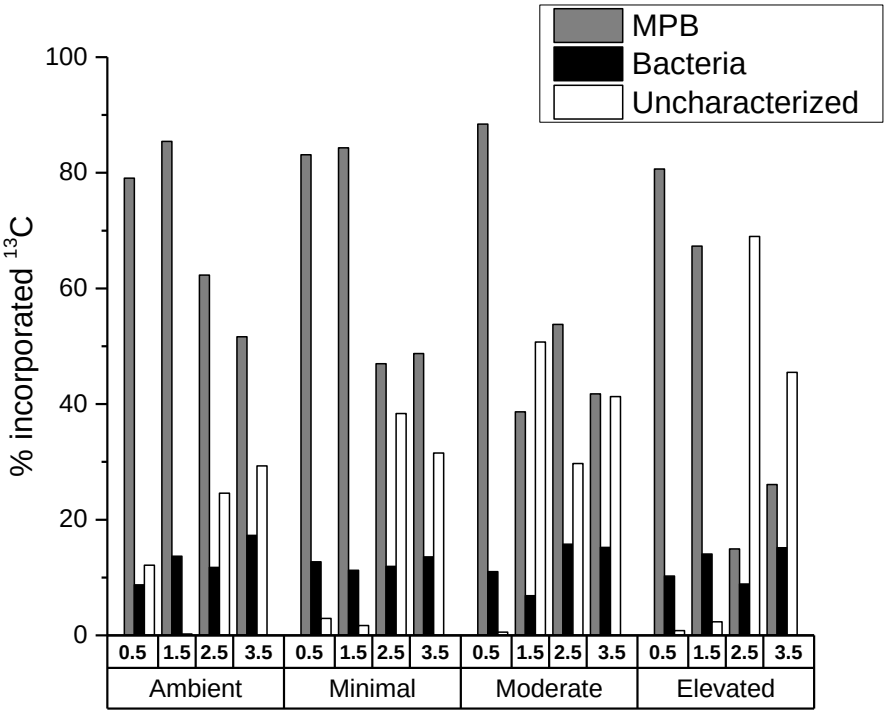

940

941 **Figure 3:** Excess ^{13}C incorporation into microphytobenthos, bacteria, and uncharacterized OC
942 as a percentage of ^{13}C contained in sediment OC in 0-10 cm. There are no error bars as PLFAs
943 were analyzed for only one replicate sample from each time period.

944

Biogeosciences Discuss., https://doi.org/10.5194/bg-2017-448
Manuscript under review for journal Biogeosciences
Discussion started: 2 November 2017

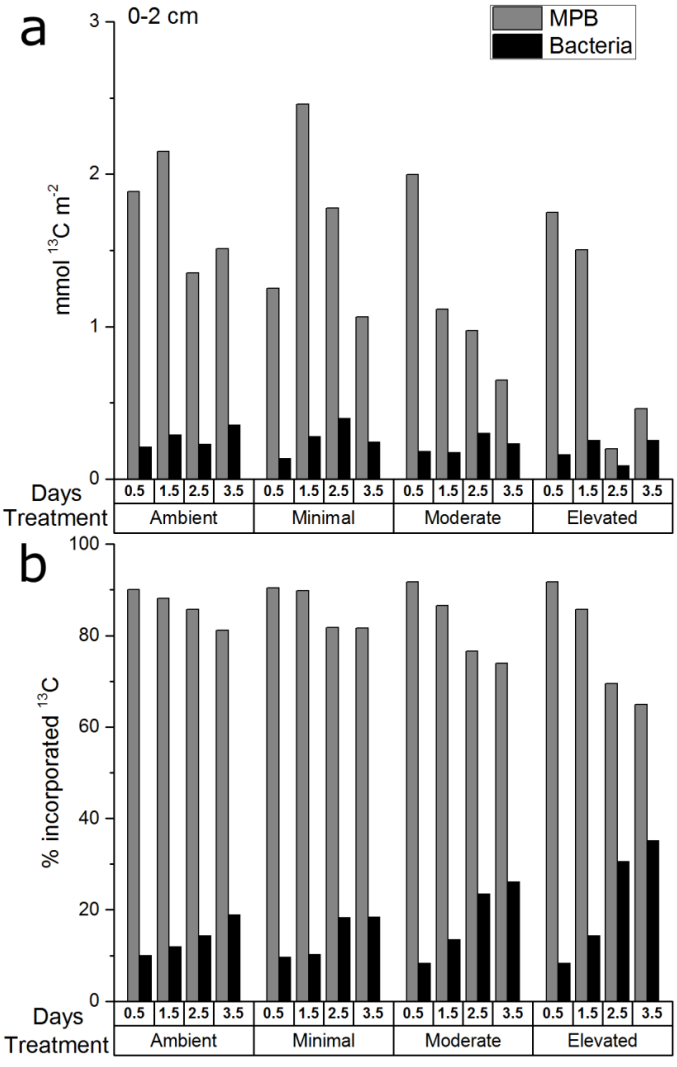

Figure 4: ^{13}C within MPB and bacterial biomass in sediment at 0-2 cm depth as A) total excess ^{13}C (mmol ^{13}C m^{-2}) and B) a percentage of the total ^{13}C in microbial biomass at 0-2 cm at each time period. There are no error bars as PLFAs were analyzed for only one replicate sample from each time period.

Biogeosciences Discuss., https://doi.org/10.5194/bg-2017-448
Manuscript under review for journal Biogeosciences
Discussion started: 2 November 2017

950

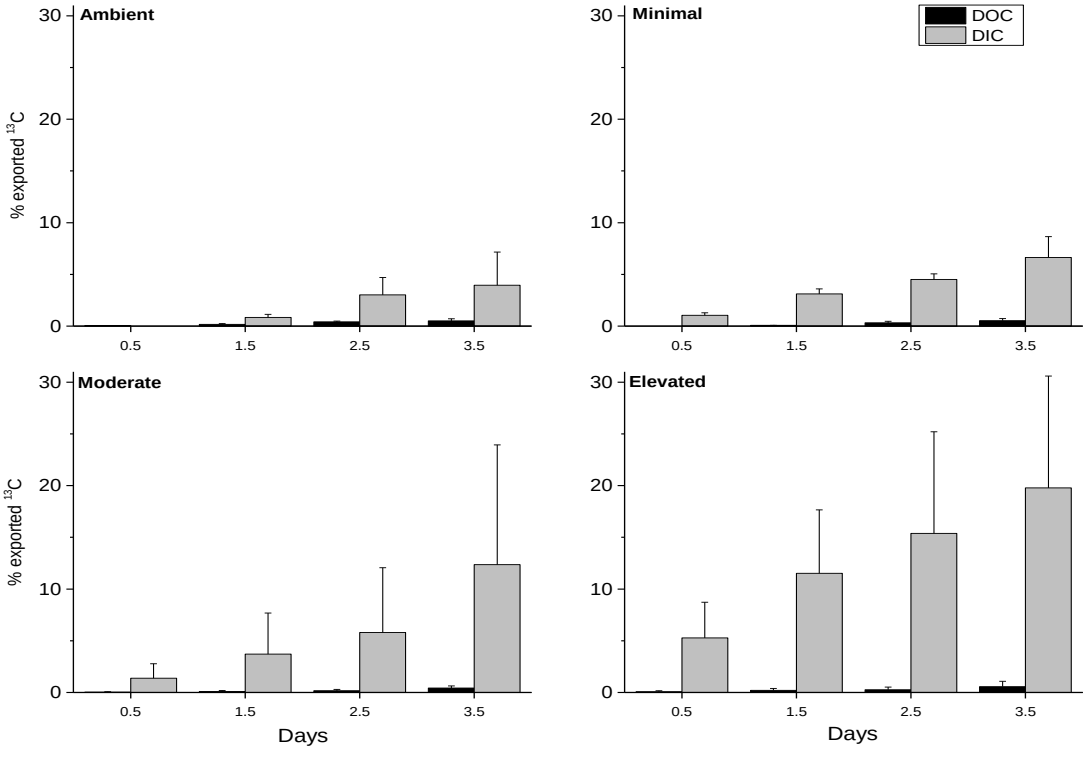

951

952 **Figure 5**: Effluxes of ^{13}C from the sediment as dissolved organic carbon (DOC) and dissolved
953 inorganic carbon (DIC) as a percentage of the total ^{13}C contained in sediment at 0-10 cm
954 depth at each sampling time (mean ± SE).

Biogeosciences Discuss., https://doi.org/10.5194/bg-2017-448
Manuscript under review for journal Biogeosciences
Discussion started: 2 November 2017

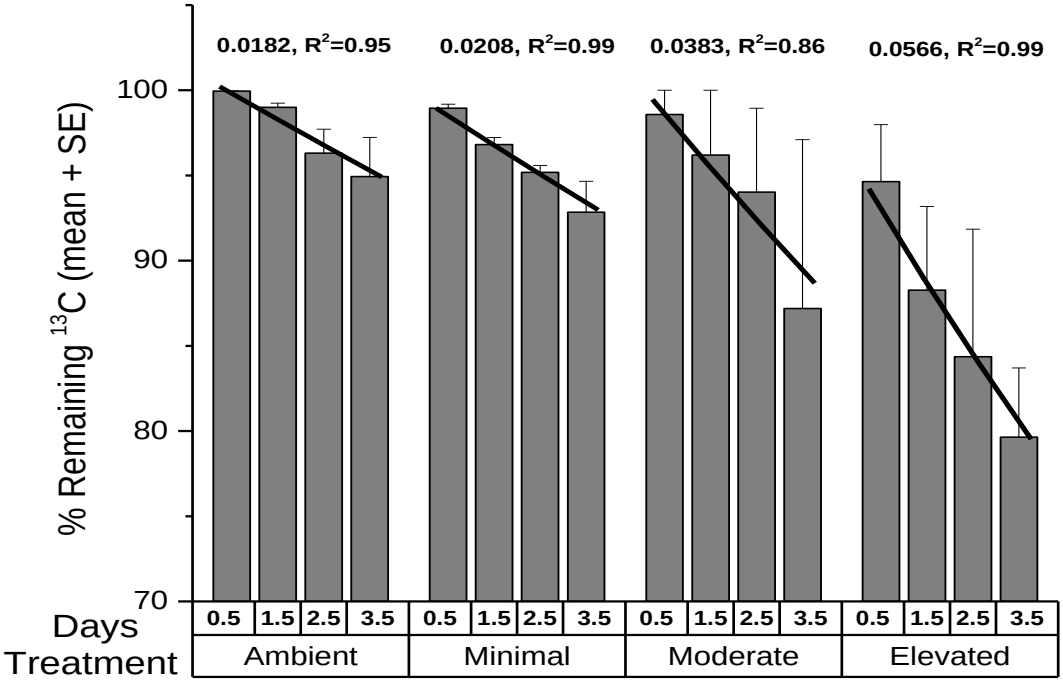

955

956 **Figure 6**: The percentage of ^{13}C remaining in sediment OC (0-10 cm depth) after accounting

957 for losses of $DI^{13}C$ and $DO^{13}C$ to the water column (mean ± SE). Lines are exponential decay

958 functions for each treatment across the 3.5 d of incubation (Loss rate constant, R^2 of function).

Biogeosciences Discuss., https://doi.org/10.5194/bg-2017-448
Manuscript under review for journal Biogeosciences
Discussion started: 2 November 2017

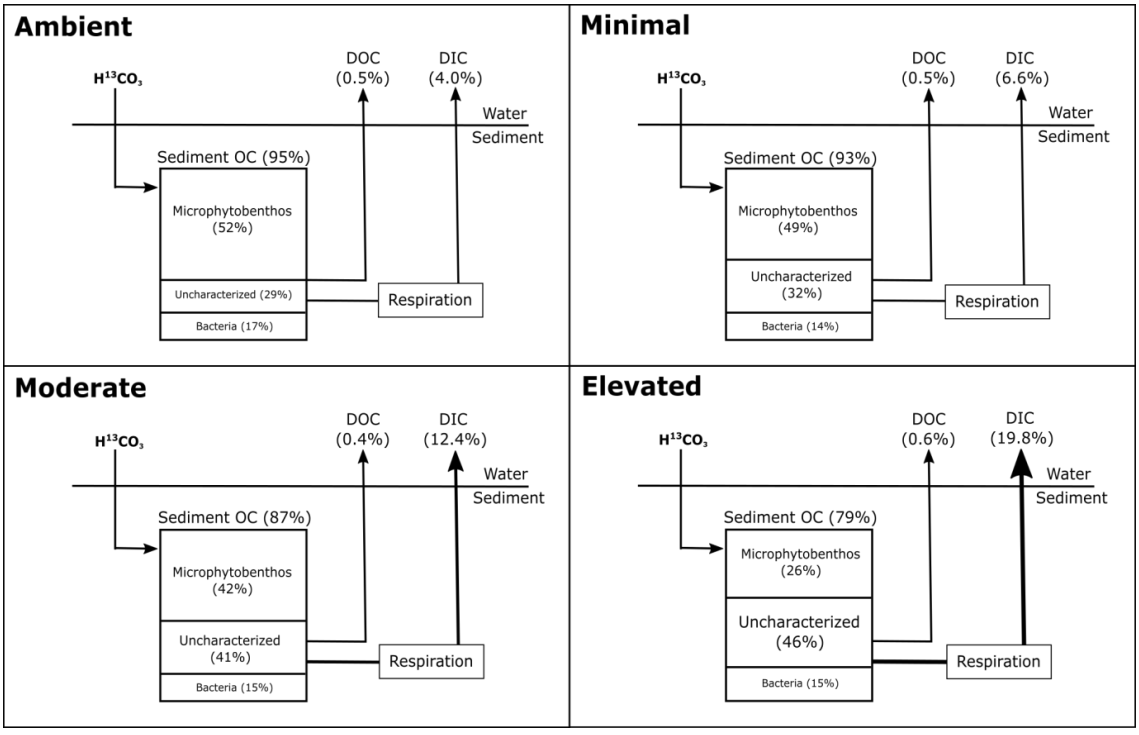

Figure 7: Distribution of ^{13}C at 3.5 d of incubation of inundated sediment including loss pathways for DIC and DOC. The ^{13}C contained in sediment organic carbon (sediment OC) is further partitioned into microphytobenthos, bacteria, and uncharacterized organic carbon as a percentage of the ^{13}C in sediment organic carbon at 0-10 cm 3.5 d after labeling (Figure layout from Eyre et al., 2016).